

Atom motions of copper dissolved in lead-tin alloys

C.-K. Hu and H. B. Huntington

Department of Physics, Rensselaer Polytechnic Institute, Troy, New York 12181

G. R. Gruzalski

Solid State Division, Oak Ridge National Laboratory, Oak Ridge, Tennessee 37830

(Received 28 January 1983)

The diffusion and electromigration of copper in lead-tin alloys containing up to 12 at. % Sn have been studied for sample temperatures between 100 and 317°C. The diffusion measurements were made by the standard sequential-sectioning technique, adapted to the 12.8-h half-life of the isotope ^{64}Cu . The rapid decrease of copper diffusivity with increasing concentration of tin is interpreted as evidence for trapping with a binding energy of about 0.3 eV. Purity of the lead solvent proved to be very important in measuring the low-temperature diffusivity. Although our values of the copper diffusivity in "pure" lead are slightly higher than other reported values, our Arrhenius curves tend to fall at the lowest temperatures, showing the effect of trapping by minute amounts of unwanted impurities. The solubility of copper in the lead and in the lead-tin alloys was determined from those diffusion measurements where the surface concentration exceeded the solubility limit. One feature which is still under investigation is that, at low temperatures, the diffusivity as a function of tin content goes through a minimum and then increases perceptibly. The electromigration results were obtained by the steady-state method. The effective charge number for copper was determined to be about unity, independent of tin concentration. In other words, the electromigration force on the mobile atoms is unchanged by the trapping phenomenon, although, of course, the time to reach equilibrium is prolonged.

I. INTRODUCTION

The so-called "fast-diffuser" systems have evoked considerable interest¹ because of their rather unusual behavior in regard to atom-movement phenomena. In particular, dilute solutions of noble metals, transition metals, and divalent metals in lead have been extensively studied.²⁻⁵ In addition to measurements of diffusion, there have been studies of self-diffusion enhancement by impurities,^{2,6} of internal friction behavior,^{7,8} of the isotope effect in diffusion,^{9,10} of the influence of pressure,¹¹⁻¹⁴ of the interstitial and substitutional distribution of the solute,¹⁵ and of the response to high electric currents (electromigration).¹⁶⁻²⁰ As an outgrowth of these last studies, this laboratory has become involved in measuring atom movements (diffusion and electromigration) of various fast diffusers in lead-tin solders as a function of temperature and composition.

The first report of this work²¹ (referred to hereafter as I) concerned the metallic impurities, silver and nickel. The temperature range was from 150°C to 300°C, and the composition was from 0 to 12 at. % Sn in lead. The findings for the two metal solutes were quite different. The diffusivity of the silver D_{Ag} increased with the addition of tin so that D_{Ag} at 230°C more than doubled with the addition of 12 at. % Sn. The effective charge number of the silver Z_{Ag}^* , which measures the strength of the electromigration drive,²² decreased from about +1 in pure lead to a small negative value for the alloy with 12 at. % Sn. On the other hand, the diffusivity of the nickel dropped very rapidly with the addition of tin. The tin ions act apparently as very deep traps with binding energy of the order of 1 eV.

From the few valid measurements that it was possible to make of the electromigration, it appeared that the trapping had little effect on the effective charge number of the nickel, Z_{Ni}^* . This result is consistent with a picture in which the trapped atoms make a negligible contribution to the electromigration flux, and the local equilibrium between trapped and untrapped nickel atoms is maintained throughout the anneal.

We report here an investigation of the behavior of copper atoms in the same lead-tin alloys. There is some similarity to the case of nickel in that there is again evidence of trapping by the tin, but the binding energy is much lower—0.3 eV. There are, however, the following interesting new features that merit special consideration.

(1) The copper has an especially high mobility and low solubility in the lead. It was possible to determine the solubility from those measurements in which the final surface concentration exceeded the solubility limit.

(2) The diffusivity of copper is markedly sensitive to minute amounts of impurity at lower temperatures as indicated by the curvature of the Arrhenius plots for "pure" lead when extended into this region. Many of the diffusion measurements were repeated with a view to maintaining as pure a solvent matrix as possible. As will be discussed later, however, it appears that with all the precautions available, it was not possible to completely eliminate some trace impurity actively trapping the copper at low temperature.

(3) The low solubility of the copper made it infeasible to work at the lower temperatures with the low specific activity (2 Ci/g upon delivery) of the commercial isotope ^{64}Cu . In due course, three shipments from the Oak Ridge National Laboratory with activities of about 150 Ci/g

upon delivery, allowed us to extend measurements 100°C lower in temperature.

(4) For $T \leq 200^\circ\text{C}$ the plots of D_x/D versus tin concentration x showed a quite peculiar feature. (Here D_x and D are the diffusivity of copper in lead for x and for 0 at. % Sn, respectively.) These plots fell by an order of magnitude during the first few percent of alloying, but with additional tin D_x/D came to a minimum, and thereafter increased to a maximum—or possibly to a constant value at the end of the composition range under study. The explanation of this unexpected effect is a challenging problem which we can discuss only qualitatively at this time.

II. EXPERIMENTAL PROCEDURE

The diffusion measurements were carried out by a standard sequential-sectioning technique using the radioisotope ^{64}Cu . The electromigration results were obtained by steady-state measurements, whereby specimens with initially uniform distribution of the ^{64}Cu were subjected to annealing with high dc currents for times long enough to attain the steady-state distribution. Many of the steps in the experimental procedure that were described in I apply here unchanged. Points of difference arise from the specific isotope used.

The radioactive ^{64}Cu source was supplied as copper nitrate in a $\sim 1N$ solution of nitric acid. The radioactive solution was allowed to evaporate, and then about 10 ml of deionized water was added to the copper nitrate. A small portion of this solution was diluted with deionized water, forming a plating solution of about 100 μCi . Plating was effected by bringing a freshly etched face of the specimen into contact with the surface of the solution; to ensure that only the specimen face was plated, the specimen was raised from the solution until contact between the face and meniscus was as close as possible. After a few minutes plating time, the specimen was rinsed with water, methanol, and acetone, and dried with Kimwipes. The resulting source strength deposited on the sample was 1–10 μCi . After the plating the experimental procedure was essentially the same as described in I. For diffusion runs, however, two additional oil-immersion furnaces were constructed with constant mechanical stirring and a flow of a reducing gas (25 wt. % H_2 –75 wt. % He). For electromigration the samples initially had a uniform distribution of copper whose concentration was well below the solubility limit.

The diffusion and electromigration anneals, the sequential sectioning, and the weighing and the counting of the radioactivity have all been described in I. There was one complication in the analysis of the diffusion runs which did not occur earlier. While the higher-temperature studies were ordinarily performed shortly after the isotope shipment arrived, and the studies used material of high specific activity, those measurements performed at lower temperatures required the longer anneal times and hence used the isotope at lower levels of specific activity. To maintain the counting rates at a suitable level, these lower-temperature runs required a higher concentration of copper (active + inactive) so that the solubility limit at the surface was often exceeded. In these cases the Gaussian thin-film solution shown in Fig. 1(a), which worked

very well for the early high-temperature runs, was no longer satisfactory. Instead, one fitted the data appropriately to the complimentary error-function solution. An added dividend in this procedure was that one could obtain the solubility from the fitting parameters. In Fig. 1(b), we show examples of both Gaussian and complimen-

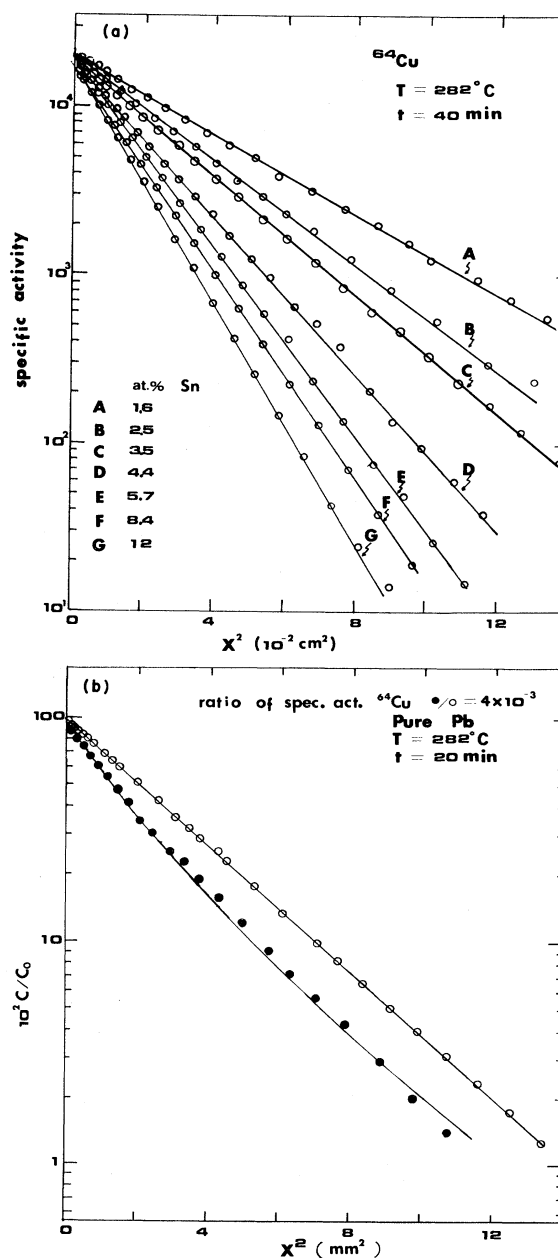


FIG. 1. (a) Diffusion penetration profiles of copper in PbSn alloys. (b) Diffusion penetration profiles of copper in pure lead. The specific activity of the copper corresponding to the solid circles is 4×10^{-3} of that corresponding to the open circles. The upper and lower curves, respectively, are a Gaussian and an error-function fit to the appropriate data.

tary error-function fitting for copper diffusion in pure lead at temperature $T=282^\circ\text{C}$. The initial sections gave high points because of trapping in the oxide layer. The corresponding data have been omitted in Figs. 1(a) and 1(b).

III. RESULTS OF MEASUREMENTS

A. Diffusion studies

A considerably larger number of measurements of diffusion were performed than were minimally needed to define the variation of the copper diffusivity with temperature and composition. A certain amount of duplication resulted, first because of repeating measurements with the high-specific-activity ^{64}Cu from the Oak Ridge National Laboratory, and second because of the growing realization of the importance of high purity in the basic lead solvent. This realization led us to procure lead of 99.9999% purity in place of that of 99.999% purity, to use graphite molds to form the specimens, and to homogenize the specimens in fused-quartz rather than Pyrex ampoules. Rather than presenting all the data in what follows, which would lead to some confusing duplication, we shall concentrate on the results obtained with 99.9999%-purity material, maintained as pure as we were able and impregnated with the high-specific-activity isotope. In due course the effects of the higher purity and higher specific activity will be pointed out.

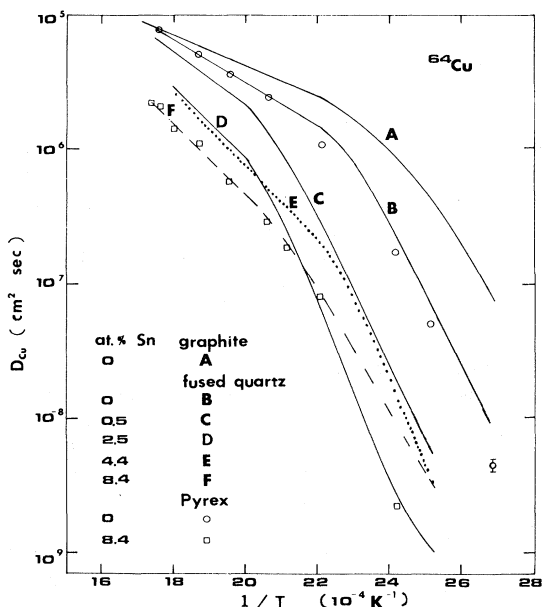


FIG. 2. Arrhenius plots of the diffusivity of the copper in pure lead and lead-tin solders. The curves are smooth lines drawn through the data (not shown). Curve *A* is for the samples prepared by melting and casting in a graphite crucible. The other curves are for specimens grown in fused quartz. The individual data points represent results obtained with 99.9999%-purity lead: ○ for zero tin (close to *B*) and □ for 8.4 at. % Sn (mostly close to *F*).

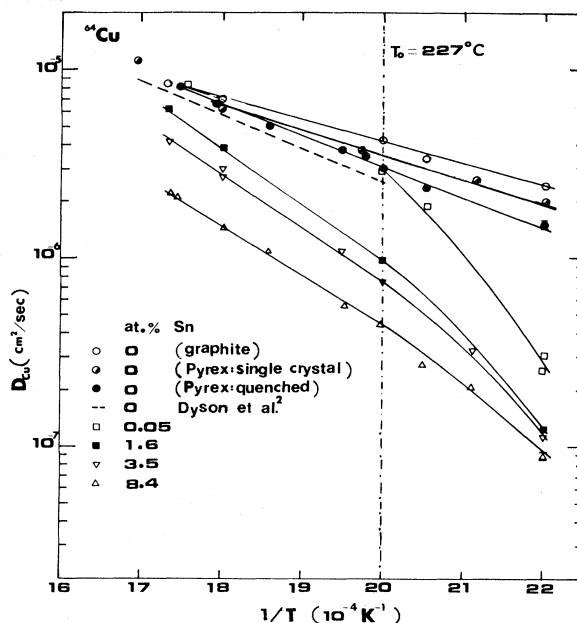


FIG. 3. Diffusivity of copper in lead and lead-tin solders as a function of inverse temperature for temperature above 180°C . The straight lines are least-squares Arrhenius fits.

We note the following.

(i) The behavior of the copper diffusivity D_{Cu} as a function of T^{-1} for various compositions is shown in Fig. 2. None of the curves are straight Arrhenius lines but all drop downwards as the lower temperatures are approached. This is true to some extent for even the "purest" lead. This curvature is the consequence of the trapping interaction between the copper and the tin and/or whatever other impurities are present, as will be discussed later. Another interesting feature which also requires later comment is the tendency of the lines for the alloys of higher tin content to cross at lower temperatures.

(ii) The effect of maintaining higher purity in the solvent lead is also displayed in Fig. 2, where results with the 99.9999%-purity lead are compared with two sets of those obtained originally with 99.999%-purity lead. The copper diffusivity in the samples made from 99.9999%-purity lead grown in fused quartz is higher than it is in samples made from 99.999%-purity lead grown in Pyrex for $T \leq 180^\circ\text{C}$. These diffusivities are about the same for $T > 180^\circ\text{C}$. This result suggests that more impurities were introduced in the samples grown in Pyrex than in fused quartz. Samples grown in Pyrex were sent to several places for impurity analysis. The neutron activation study at Oak Ridge National Laboratory showed that the most abundant impurity in the 99.999%-purity lead was iron, with a concentration of about 20 at. ppm. However, the mass-spectrometer analysis from the IBM Yorktown Heights Laboratory indicated that the samples contained 15–70 at. ppm Fe, ~400 at. ppm K, ~200 at. ppm Na, and ~90 at. ppm Si. These impurities probably also act as trapping sites for copper which cause nonlinear behavior in Arrhenius plots even in "pure" lead.

Figure 3 shows Arrhenius plots for Pb and PbSn alloys

with different sample preparations for temperatures above 180°C. The diffusivities were fitted to the usual expression $D_0 \exp(-Q/kT)$, and the straight lines going through the pure lead data are fits to this expression over the temperature ranges shown, as are the straight lines going through the alloy data for $T > 227^\circ\text{C}$. The four curves through the alloy data for $T < 227^\circ\text{C}$ were drawn to guide the eye, and the fit of Dyson *et al.*² has been included for comparison. The activation energies Q and the preexponential factors D_0 obtained from the fits are shown in Table I. As can be seen, the activation energy Q from lead melted in graphite molds is about 30% lower than that of lead melted in fused-quartz or Pyrex tubes.

(iii) Figure 4 shows the results obtained for the solubility of Cu in lead as a function of temperature, in comparison with the values of earlier workers.^{10,18} These solubilities result from those runs for which the surface concentration is always above the solubility limit. In this case the boundary condition is that of a fixed concentration at the actual lead surface and the appropriate solution is that of the complementary error function

$$C(x,t) = C_0 \{ 1 - \text{erf}[x/(4Dt)^{1/2}] \}, \quad (1)$$

where C_0 is the concentration of copper at the solubility limit for the appropriate sample temperature. An identification of C_0 requires that one knows the specific activity of the isotope as determined from a fixed time in the past and the relative efficiency of the counting technique. The data are then fitted to Eq. (1) for best values of C_0 and D . The solubility of copper in Pb and PbSn alloys was found to be $C_0 = (3.6 \pm 3.6) \times 10^{-3} \exp[-(0.35 \pm 0.05) \text{ eV}/kT]$ weight fraction. The large uncertainty of the solubility determined in this manner (see Fig. 4) is due to the large uncertainty of the specific activity. Also the oxidation layer on the surface of the samples probably contributes to the scatter in our values.

(iv) In I a simple trapping theory was sketched which predicted

$$\frac{D - D_x}{xD_x} = ze^{-g/kT}, \quad (2)$$

where D_x and D are, respectively, the diffusivity in the alloy at tin concentration x and in pure lead, z is the number of trapping sites per tin atom, and g is the free energy for the trapped complex. It is assumed that the number of traps considerably exceeds the number of mobile impurities. Equation (2) predicts that $(D - D_x)/(xD_x)$ should be independent of x , which is reasonably well borne out for the case of copper in lead alloys as shown in Fig. 5. The data fit rather well to a straight line for $T \geq 240^\circ\text{C}$ whose slope gives a binding energy for trapping of $0.32 \pm 0.07 \text{ eV}$ and an entropy of $-(4.8 \pm 1.4)k$, assuming $z=6$. The marked scatter at lower temperatures arises from an effect discussed in the next paragraph.

(v) It has been remarked that the lines in Fig. 2 cross at the lower temperatures. The same behavior is displayed somewhat more clearly in Fig. 6 where the diffusivity is plotted versus the tin concentration x for various temperatures. At low temperatures the diffusivity goes through a minimum versus x and either shows a subsequent maximum or stabilizes at a constant value. This rather remarkable behavior seems to be explicable possibly on the

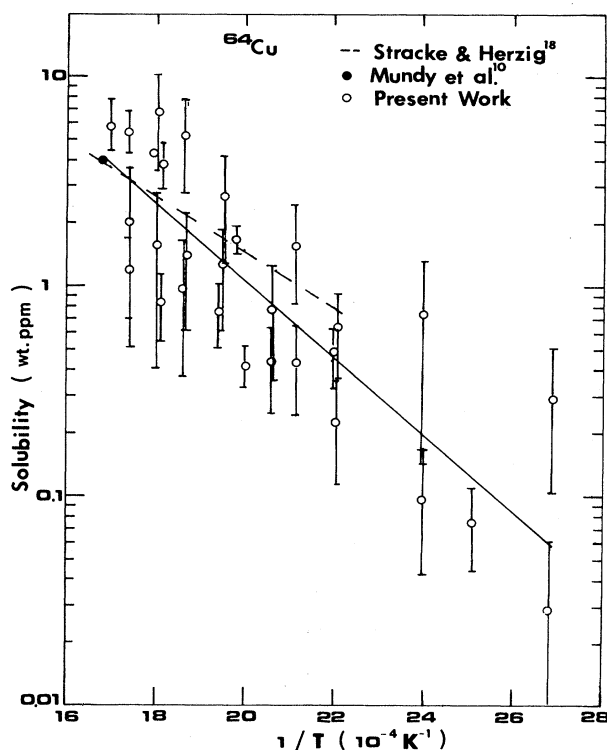


FIG. 4. Solubility in wt. ppm of copper in Pb and PbSn alloys as a function of T^{-1} . The solid line is a least-squares fit to the present data.

basis that the higher concentrations of tin form complexes which actually aid the diffusion of the copper by passing the trapped atoms along from one tin atom to another. We are in the process of trying to devise a more detailed theoretical model which could fit with these observations.

B. Electromigration

As in the case of the nickel as mobile impurity (I), it appears that the trapping has little effect on the electromigration drive as measured by the effective charge number for copper Z_{Cu}^* . However, the presence of the tin does complicate the process of measurement since it appears to accelerate the motion of the copper to the surface, as shown by the inconclusive data taken at $T=220^\circ\text{C}$ (Fig. 7). Presumably the tin allows oxygen to penetrate the alloy more easily and to draw out the copper. Shortening the time of the experiment, or using a reducing gas, appear to be possible ways to minimize this undesired effect which becomes particularly severe in runs of long duration. The electromigration profiles for copper in Pb-50 at. ppm Sn and Pb-4.4 at. % Sn are also shown in Fig. 7 and yield reliable Z^* measurements. The value of Z^* for copper in Pb-4.4 at. % Sn is 0.8 ± 0.2 at $T=258^\circ\text{C}$ and is close to 1.1 ± 0.2 for copper in Pb-50 at. ppm Sn. For pure lead the literature^{18,23} gives 1.0 ± 0.1 for Z_{Cu}^* .

TABLE I. Activation energies Q and preexponential factors D_0 for copper in pure lead and lead-tin solders.

| x (at. % Sn) | Q (eV) | D_0 (cm ² /sec) | T (°C) |
|-------------------|-----------------|--------------------------------|----------------------|
| 0 | 0.23 ± 0.01 | $(8.7 \pm 1.2) \times 10^{-4}$ | 180–304 ^a |
| 0 | 0.28 ± 0.02 | $(2.3 \pm 1.3) \times 10^{-3}$ | 180–282 ^b |
| 0 | 0.32 ± 0.01 | $(4.6 \pm 0.8) \times 10^{-3}$ | 180–282 ^c |
| 0 | 0.24 ± 0.01 | $(8.0 \pm 6.0) \times 10^{-4}$ | 218–300 ^d |
| 0 | 0.35 ± 0.02 | $(7.9 \pm 2.0) \times 10^{-3}$ | 227–316 ^e |
| 1.6 | 0.61 ± 0.02 | (1.3 ± 1.4) | 227–304 ^f |
| 3.5 | 0.56 ± 0.03 | $(3.1 \pm 1.9) \times 10^{-1}$ | 227–304 ^f |
| 8.4 | 0.52 ± 0.02 | $(7.6 \pm 3.1) \times 10^{-2}$ | 227–304 ^f |

^aObtained from the samples prepared by melting and casting the lead in graphite.

^bObtained from lead by melting in Pyrex and crystal grown by Bridgman technique.

^cObtained by melting lead in Pyrex or fused quartz.

^dObtained from Ref. 13.

^eObtained from Ref. 2.

^fObtained by melting and casting lead-tin solders in fused quartz.

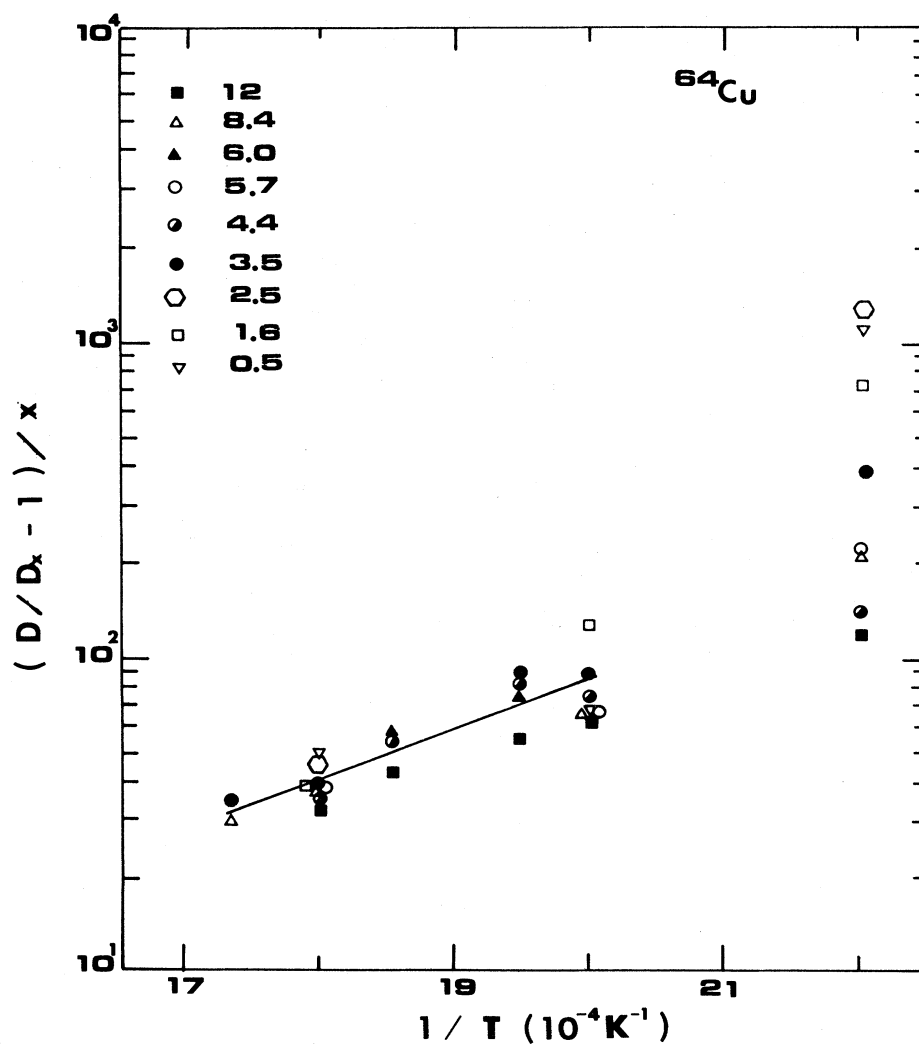


FIG. 5. Plot of $(D/D_x - 1)/x$ vs $1/T$ for copper in $PbSn$ alloys. The line is a least-squares fit to Eq. (2) for $T \geq 240^\circ\text{C}$.

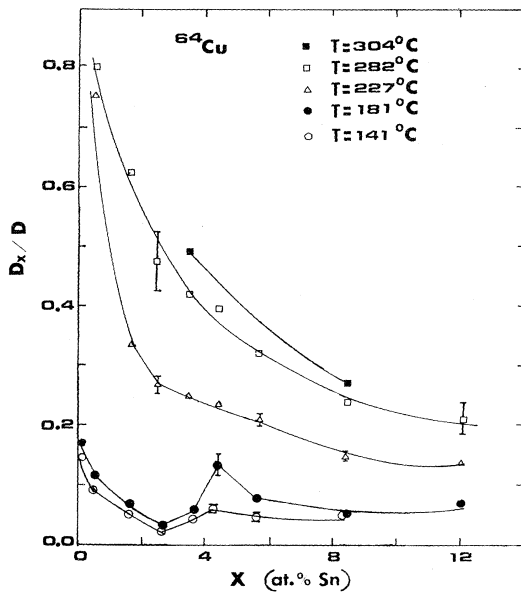


FIG. 6. Ratio of D_x/D as a function of the tin composition. Lines have been drawn to guide the eye.

IV. SUMMARY

The investigation of the diffusion and electromigration of copper dissolved in the lead-tin solders has revealed several interesting effects.

(1) As in the case for a similar study of nickel in these solders, the copper atoms are strongly trapped by tin. However, the tin-copper binding energy is of the order of 0.3 eV, which is appreciably smaller than the tin-nickel binding energy.

(2) The copper diffusivity D_{Cu} is sensitive to very small concentrations of impurities. This was particularly evident in the curvature of the Arrhenius plot for copper in pure lead. All the precautions we took to maintain the purity of the basic lead solvent (99.9999%-purity lead, graphite crucibles, and fused-quartz ampoules) did not suffice to completely eliminate this effect.

(3) With the higher isotope concentrations needed to measure diffusion at low temperature, it was possible to determine the copper solubility from fitting the penetration plot to a complimentary error-function solution. The results are in reasonable agreement with measurements by other investigators.

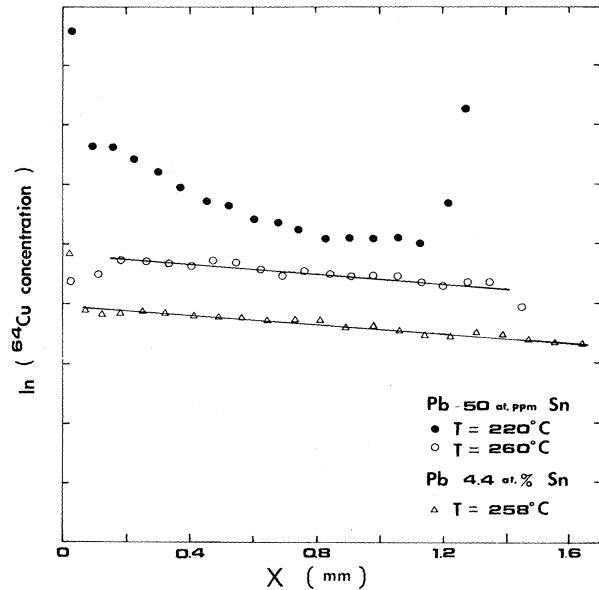


FIG. 7. Electromigration profiles of copper in lead-tin alloys. Surface end effect is large for $T=220^\circ\text{C}$.

(4) The copper diffusivity decreases rapidly with increasing tin concentration x_{Sn} . For low sample temperatures, D_{Cu} vs x_{Sn} exhibits a minimum followed by a maximum or perhaps a constant value as x_{Sn} increases. The only apparent explanation is that this increase in D_{Cu} with increasing x_{Sn} must be the result of the trapped copper being passed along from one tin atom to the next.

(5) The presence of the tin has little effect on the electromigration of the copper as measured by Z^* .

ACKNOWLEDGMENTS

We gratefully acknowledge the support of the IBM Research and Development Facility at East Fishkill, New York. We also wish to thank the Division of Materials Sciences, Office of Basic Energy Sciences, U. S. Department of Energy, under Contract No. W-7405-eng-26 with Union Carbide Corporation for partial support. We are also indebted to the IBM Thomas J. Watson Laboratory for analysis of impurities in our samples by mass spectrometer. We are grateful to Messalina Wang and Donald Yeh for technical assistance.

¹W. K. Warburton and D. Turnbull, in *Diffusion in Solids: Recent Developments*, edited by A. S. Nowick and J. J. Burton (Academic, New York, 1974), Chap. 4.

²B. F. Dyson, T. Anthony, and D. Turnbull, *J. Appl. Phys.* **37**, 2370 (1966).

³G. V. Kidson, *Philos. Mag.* **13**, 247 (1966).

⁴C. T. Candland and H. B. Vanfleet, *Phys. Rev. B* **7**, 575 (1973).

⁵R. A. Ross, H. B. Vanfleet, and D. L. Decker, *Phys. Rev. B* **2**, 4026 (1974).

⁶J. W. Miller, *Phys. Rev. B* **2**, 1624 (1970).

⁷T. J. Turner, S. Painter, and C. H. Nielsen, *Solid State Commun.* **11**, 577 (1972).

⁸C. H. Nielsen and T. J. Turner, *Solid State Commun.* **15**, 243 (1974).

⁹J. W. Miller, J. N. Mundy, L. C. Robinson, and R. E. Loess, *Phys. Rev. B* **8**, 2411 (1973).

¹⁰J. N. Mundy, J. W. Miller, and S. Rothman, *Phys. Rev. B* **10**, 2275 (1974).

¹¹A. Ascoli and D. Poletti, *Phys. Rev. B* **6**, 3681 (1972).

¹²J. A. Weyland, D. L. Decker, and H. B. Vanfleet, *Phys. Rev.*

- B 4, 4225 (1971).
- ¹³C. T. Candland, D. L. Decker, and H. B. Vanfleet, Phys. Rev. B 5, 2085 (1972).
- ¹⁴D. L. Decker, C. T. Candland, and H. B. Vanfleet, Phys. Rev. B 11, 4885 (1975).
- ¹⁵G. R. Gruzalski, Solid State Commun. 34, 539 (1980).
- ¹⁶C. Herzig and E. Stracke, Phys. Status Solidi A 27, 75 (1975).
- ¹⁷M. Y. Hsieh, H. B. Huntington, and R. N. Jeffery, Cryst. Lattice Defects 7, 9 (1977).
- ¹⁸E. Stracke and C. Herzig, Phys. Status Solidi A 47, 513 (1978).
- ¹⁹D. A. Golopentia and H. B. Huntington, J. Phys. Chem. Solids 39, 975 (1978).
- ²⁰H. Nakajima and H. B. Huntington, J. Phys. Chem. Solids 42, 171 (1981).
- ²¹C.-K. Hu and H. B. Huntington, Phys. Rev. B 26, 2782 (1982).
- ²²The force of electromigration may be expressed as $F_a = |e|EZ^*$, which is the defining equation for the dimensionless effective charge number Z^* . Here E is the applied electric field and e is the electron charge.
- ²³M. F. Hsieh and H. B. Huntington, J. Phys. Chem. Solids 39, 867 (1978).